euspen's 23rd International Conference & Exhibition, Copenhagen, DK, June 2023
www.euspen.eu

Dynamical simulation of an under-actuated surface composed by spherical rotors during sorting operations

Edoardo Bianchi[1], Oliver J. Jorg[2], Gualtiero Fantoni[2], Francisco Javier Brosed Dueso[1], José A. Yagüe Fabra[1]

[1]*University of Zaragoza, Department of Design and Manufacturing Engineering, Calle Maria de Luna 3, 50018 Zaragoza*
[2]*University of Pisa, Department of Civil and Industrial Engineering, Largo Lucio Lazzarino, 56122 Pisa*

ebianchi@unizar.es

Abstract
In the field of materials handling, research continues to focus on modular and flexible systems to adapt to market requirements. With this in mind, but also with a view to reducing costs and simplifying design and control, a new under-actuated modular device is proposed. The latter, combined with other modules, creates surfaces that can be used for orienting, stopping, slowing down and sorting materials. The proposed device consists of a spherical rotor whose axis of rotation is defined in certain predetermined directions in the transport plane. The module's missing actuation is compensated for by gravity or by the initial velocity possessed by the manipulated body, while the temporary definition of the axis is obtained by magnetising ferromagnetic pins acting on the sphere with solenoids. The article focuses on the use of the device for sorting, one of the main applications of the system. In order to demonstrate the use of the concept, a dynamic simulation of a rectangular array of modules during the above-mentioned activity and the results associated with it are presented. In particular, the simulation focuses on the dynamics of the spherical rotors and the contact with the pins that generate the temporary rotation axis.

Under-actuation, Material handling, Sorting, Dynamic simulation

1. Introduction

The handling and transport of materials within companies and warehouses are always topics of interest in scientific research, as the market demands to continuously increase the flexibility and efficiency of these processes [1]. In particular, the focus of the research is on the main handling activities such as sorting, slowing, stopping, positioning and orientation of the material flow. With these aims in mind, various types of systems have been studied, among which programmable surfaces are an important section. These systems are generally modular surfaces that utilise vibrations [2], pressurised air [3], ciliary motion [4], variable morphology of modules [5] or rotors [6, 7] to move material. Focusing on the last category, i.e. surfaces composed of rotors, it was noted that the existing systems consist of modules containing several motorised wheels [6] or one wheel [7] with at least two motors, one for rotation around the spinning axis and the other to orientate the same axis in the plane. In contrast, there is a lack of simplified systems without motors to perform the same tasks. For this reason, in the following article, the concept and analyses proposed by the authors focus on a surface composed of modules with under-actuated rotors that exploit gravity or the velocity already possessed by an object to manipulate objects during their motion. In addition to this, in order to further simplify the design and control, the only actuation of the rotor is discrete and consists of the orientation of its axis of rotation in certain predefined directions. The paper focuses on the correct modelling of this handling system and on its possible application for sorting purposes. This is done through simulations conducted with the well-known software for multi-body dynamics, *Hexagon D&E Adams MSC*, whose model and parameters are here presented. Specifically, the simulation is exploited, firstly, to validate the analytical model proposed for the rotor, and then, to analyse the effect of the external sources of actuation on the dynamics of the sorted material. The rest of the paper is organized in the following sections: Section 2 explains the concept, its operating principle and the analytical model, in Section 3 a multi-body dynamic model of a sorting line is illustrated, Section 4 shows the results of the simulations, in particular, the validation of the analytic model and the effect of the different actuation sources. Finally, Section 5 states the conclusions.

2. Description of the surface concept

The surface proposed by the authors consists of independent modules, each containing an idle rotor whose rotation axis orientation can be controlled. The rotors thus defined can generate a programmable friction field used to manipulate an object passing over the surface. Since the operation of the surface is based on the friction forces of the individual modules, the functioning of the rotor and its analytical model are now presented.

2.1. Concept working principle

The module developed by the authors consists of a spherical rotor surrounded in the mid-plane by semi-axes (or pins) positioned in an equispaced manner. Each pair of opposite pins constitutes a possible axis of rotation that can be selected by connecting or not connecting the pins to the sphere (Fig. 1). The axis selection is limited to a fixed number of available directions e.g. 2 (2 pin pairs) or 4 (4 pin pairs (Fig. 1)) and it is done magnetising the pins with solenoids. When the pair of solenoids is powered, pins are attracted to the sphere, otherwise they remain slightly distant. The operation of the module is based on the directions of the friction forces exchanged with an object in contact. These forces are divided into two main components, one parallel to the axis and one perpendicular. Since friction is

reduced in the perpendicular direction, being the direction in which the ball rotates, the main component of the friction forces is the one parallel to the axis.

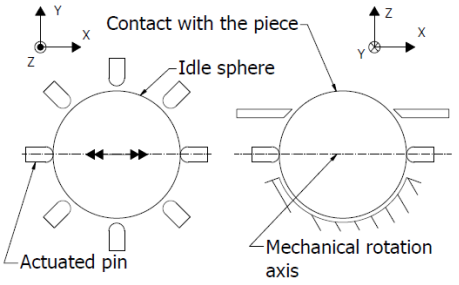

Figure 1. (Schematic illustration of the spherical concept.)

So, in summary, controlling the direction of the axis defines the parallel force and consequently the force handling the object.

2.2. Analytical model

Trying to describe the functioning of the individual module, the first step is the equlibrium of the rotor (Fig. 2).

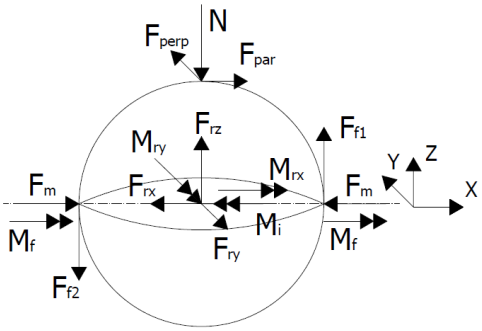

Figure 2. (Sphere's equilibrium scheme)

Where are presented the following forces:

- N, F_{par}, F_{perp}: are the forces exchanged in the contact with the object, respectively the vertical load and the two friction forces in the parallel and perpendicular direction referring to the sphere's rotation axis.
- $F_m, F_{f1,2}, M_f$: are the actions exchanged in the contact between the pin and the sphere, respectively the pressing force, the friction force and the friction torque.
- F_{rx}, F_{ry}, F_{rz}: are the reactions with the sphere support referred to the centre of the sphere, in the frame directions.
- M_{rx}, M_{ry}: are the friction torque reactions between the sphere and its support.
- M_i: is the inertial torque due to the acceleration of the sphere.

The assumption considered for the model are:

1. The contact between object and rotor is a point contact so only forces and not momentums are exchanged.
2. The forces exerted by the pins are equal and opposite and do not contribute to the traslation equilibrium.
3. Coulomb friction model: $F \leq \mu N$
4. M_{rx}, M_{ry} are at most equal to the rolling friction value of the large sphere: $M_{rx} = \mu_v N$, $M_{ry} = \mu_v N$ (μ_v rolling friction coefficient).

From the equilibrium (Fig. 2), the two friction forces, used to move the objects, result as shown in Equations (1) and (2):

$$\begin{cases} F_{par} = F_{f1} + F_{f2} + \dfrac{M_{ry}}{R} & (1) \\ F_{perp} = \dfrac{2M_f - M_i + M_{rx}}{R} & (2) \end{cases}$$

Referring back to Equation (1), considering that $F_{f1} \leq \mu_p F_m$, $F_{f2} \leq \mu_p F_m$ (Coulomb friction model with μ_p friction coefficient between pin and sphere), $M_{ry} = \mu_v N$ and that N depends on the weight of the transported object, the maximum value of the parallel force can only be controlled with F_m. For this reason, in order to have no slip between the pins and the sphere, i.e. only rotation around the *x*-axis, the value of F_m needs to be sufficiently high in relation to the load on the individual rotor. The no slip condition represents the desired and optimal operation of the rotor, since allows it to work as if its axis of rotation were defined by a mechanical component and not by contact. Equation (2), on the other hand, shows the origin of the perpendicular force, which is linked to the friction with the pins (M_f), the inertial contribution (M_i) and the rolling friction with the support (M_{rx}). The only controllable term in this case is M_f, which should be reduced in order to improve the functioning of the device. To do this, a first option is to reduce the diameter of the pin tip in contact with the ball. The second option is to support the pin so that it can rotate attached to the ball. By doing so, the friction moment M_f is the minimum between the one due to the ball-pin contact and the other generated by the rotational support of the pin. Having introduced Equation (1) and assuming that the friction force in the parallel direction also follows Coulomb's law $F_{par} \leq \mu_m N$ it is possible to determine the limiting mass ($m = N/g$) per rotor such that there is no rotation of the sphere in the *y*-direction ($F_{f1} = F_{f2} = \mu_p F_m$ e $M_{ry} \approx 0$ cautiously).

$$m_n \leq 2\frac{\mu_p \cdot \mathrm{F}_m}{\mu_m \cdot g} \qquad (3)$$

3. Multi-body dynamic simulation model

The dynamic simulation of the sorting operation in a material transport line was conducted with the software: *Hexagon D&E Adams MSC* (hereinafter "*Adams*"). In order to simplify the model without affecting the validity of the results and also to reduce simulation times, only the part of the line where sorting takes place and the bodies involved in the activity were modelled (Fig. 3). In particular, referring to Fig. 3, the elements that perform the sorting are the green spheres with yellow and magenta pins, while the cyan spheres model both the transport system before sorting and the area after it (hereinafter AAS (area after sorting)).

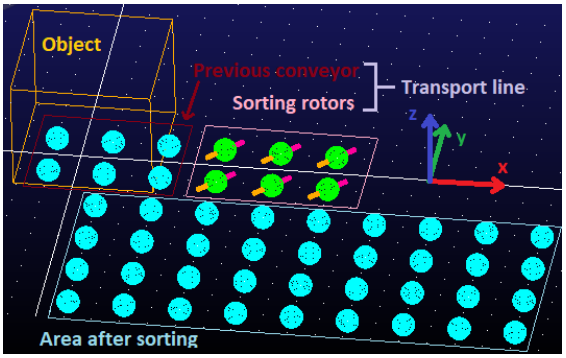

Figure 3. (*Adams* model with descriptions of the components.)

In Fig. 3, the transported object is the orange parallelepiped resting on the spheres array, *x* is the direction of line movement and *y* (negative way) is the direction of sorting. The starting

velocity of the object (in the *x*-direction), which in practice can be derived from previous conveyors or the inclination of the surface, is modelled in *Adams* by providing an initial instantaneous velocity or by varying the direction of gravity, respectively. The actuation of the pins is modelled appling forces in the direction of their axes and is active throughout the simulation. In the simulation these forces are settled on $F_m = 30\ N$ in order to verify Equation (3) and have a correct functioning of the rotors. The constraints chosen for the bodies are: a fixed joint for the cyan spheres, spherical joints for the green spheres and cylindrical joints for the pins. The contacts are between the box and the cyan spheres, between the box and the green spheres and between the green spheres and the pins. The basic parameters imposed in the *Adams* model are summarised in Table 1.

Table 1 (Parameters of the *Adams* simulation model)

Parameter	Description	Value
m	Mass of the object	5.48 kg
I_{xx}	Object inertia *x* axis	5.7 x 10^{-2} kgm^2
I_{yy}, I_{zz}	Object inertia *y,z* axis	4.7 x 10^{-2} kgm^2
m_p	Pin mass	2.0 x 10^{-3} kg
I_{xx}, I_{yy}	Pin inertia *x,y* axis	6.8 x 10^{-8} kgm^2
I_{zz}	Pin inertia *z* axis	3.9 x 10^{-9} kgm^2
r_p	Pin radius	2 mm
B x H x Z	Object dimensions	0.25 m x 0.25 m x 0.2 m
m_r	Rotor mass	0.26 kg
I_r	Rotor inertia *x,y,z* axis	4.2 x 10^{-5} kgm^2
r	Rotor radius	0.02 m
St	Stiffness contact	10^5 MPa
Dp	Damping contact	8 kg/s
Pd	Penetration depth contact	0.1 mm
Stv	Stiction transiction vel.	0.1 mm/s
Ftv	Friction transiction vel.	1 mm/s
μ_p	Friction coef. pin-rotor	0.5
μ_{max}	Friction coef. rotor-object	0.5
$\mu_{ex,surf}$	Friction coef. obj.-AAS	0.01
μ_v	Rolling friction coef. rotor	0.01 x r
μ_{rp}	Rolling friction coef. pin	0.3 x r_p

The first half of Table 1 contains all the objects parameters related to inertia and dimensions, while the second part include the parameters implemented in the contacts and in the joint friction model. The selection was done according to the suggestion of the *Adams* users guide, St, Pd are the default values, while $Dp = 8\ kg/s$ instead of $Dp = 10\ kg/s$. Stv and Ftv are smaller than the default values (respectively of $100\ mm/s$ and $1000\ mm/s$) to simulate better the stiction at low speeds. The friction coefficients are selected considering the common values for the materials in contact or the type of the latter. Taking this into account, the focus now switchs on the simulations conducted with the software. The goal is to validate the proposed analytical model and to show and compare the results of some sorting operations changing the two main initial parameters, which are foundamental for the actuation, i.e the initial velocity and the inclination of the surface. In order to achieve this with the set-up shown, 11 simulations changing the initial velocity (V_{x0}) inside the range $0.5\ m/s$ to $1\ m/s$ (with a step of $0.05\ m/s$) and 11 simulations changing the inclination of the surface (γ) from 5° to 15° (step 1°) are conducted. These ranges of inputs are compatible with normal object's velocities on a transfer line. The simulation with the initial velocity equal to $1\ m/s$ was used to collect the data for the analytic model validation too. In particular from this simulation the data are gathered from the bottom green rotor closer to the initial position of the object.

4. Results

This section contains the results of the total 22 simulations.
As introduced before, a first part concerns the validation of the analytical model, while the second one is about sorting operations and the initial parameters used.

4.1 Validation of the analytic model:

The validation consists into comparing the friction forces obtained from the dynamic simulation with the ones computable from Equations (1), (2). The first, i.e. the friction forces, are exported directly as two measures of the contact between the rotor and the object (F_{par}, F_{perp}). Instead, to calculate the analytical result counterpart, the terms exported are the ones on the right side of Equations (1), (2), i.e. F_{f1}, F_{f2}, M_{rx}, M_{ry}, M_f, M_i. These two results, for both the components (F_{par}, F_{perp}) are then plotted toghether with their absolute error to show and quantify the similarity. In Fig. 4, what has been said in the previous sentence is then illustrated. The dots represent the analytic model values and their color shows the absolute error with the *Adams* direct measure (black lines). of the two force components.

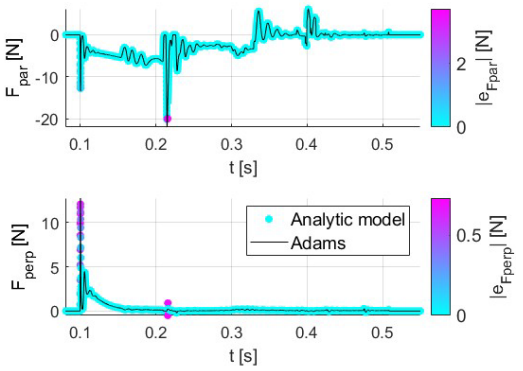

Figure 4. (F_{par} and F_{perp} obtained through *Adams* and the analytic model reported with a colored map to highlight the absolute error, zoom on the range of time where the forces are different from zero.)

As result, from Fig. 4 it appears that the analytic model predicts with a good accuracy the forces behaviour since the error is close to 0 almost everywhere. In particular, to have a reference, the absolute error is bigger than $0.01\ N$ only for the 0.48% of the simulation time ($1\ s$) for F_{par} and for the 0.46% for F_{perp}. From Fig. 4 some areas with bigger erros are visible, these occur when in the simulation there is the transiction of the contact to a new rotor. During these instants the impact brings peak values for both the results producing the slight difference. As example, the first spike with a perceivable absolute error, around $0.1\ s$, matches the first contact with the green rotor.

4.2 Sorting results with different initial conditions

The 22 sorting simulations are conducted each one varying the initial conditions which represent the actual source of motion for the object. In particular, as mentioned before, half of them exploits a different inclination of the surface, while the other half, takes as an input a previous velocity of the object, which in practice can be provided by a conveyor belt in the sorting line.
The data collected from the simulations are the displacements (linear and angular) of the object during its motion. In order to report these values in the condition of achived sorting, this limit needed to be fixed. About that, given the geometry of the system, the boundary is settled on $|y_g| = |y_{g,limit}|$, where $y_{g,limit} = H/2 + \sqrt{(B/2)^2 + (H/2)^2} = 302\ mm$ (half oh the object width plus half of its diagonal length). Then, when the displacement of the object center of mass is bigger than the limit

$|y_g| \geq |y_{g,limit}|$, the sorting is considered achieved. Taking this into account and since the *y* displacement, when the sorting is achieved, is the same for each simulation, Fig. 5 reports the x_g and θ_g displacements when the limit condition is reached.

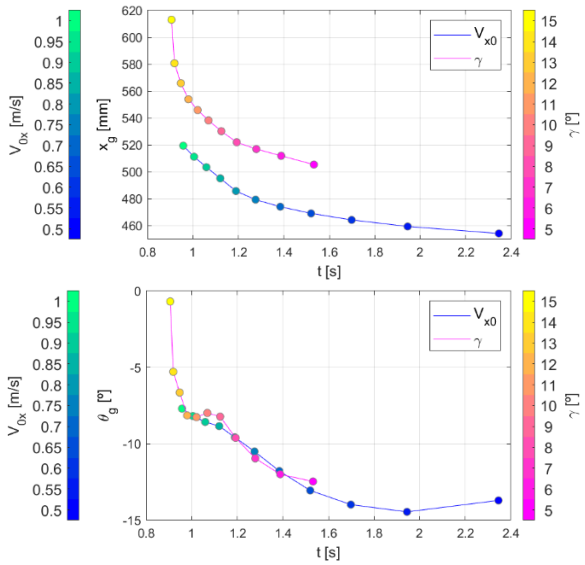

Figure 5. (x_g and θ_g displacements at the time the sorting condition is achieved, changing the initial velocity (blue plot and "cold" colored map to identificate the different velocities) and the inclination of the surface (magenta plot and "hot" colored map to identificate the different velocities) .)

As result, Fig. 5 shows that, given these plausible ranges of initial conditions and the same sorting time, the requested space in the line direction is bigger when gravity is exploited for the motion of the object. Insead, the angular displacement is similar for the two sources for a wide range of time values and when it is not, the inclination appers to modify less the original orientation. In Fig. 5 each value of x_g and θ_g displacements is identified using a colormap related to the input magnitude. This correlation evidences that, increasing both initial velocity and inclination, the sorting time and the angular displacenements decrease, while the x_g displacement grows. In addition, this effect of incrementing the space and reducing the final orientation results more evident when the input is the inclination, even if the time spent for sorting is similar to the one required for the velocity input. The trend of the angular displacement is not monotonic like the one of the x_g displacement because the resulting rotation is affected not only from the value of the forces produced by the rotors, but also from the arm of these reactions. Because of that, by varying the initial parameters, the points of the object where the rotors forces are applied differ in place and number, causing different rotations. In addition, when gravity is exploited, the distribution of the contact forces is even more variable and the orientation changes more, outside the sorting area too. Summarizing, as shown graphically in Fig. 6 and numerically by the previous Fig. 5, the sorting is achiviable with the two different input conditions and with the introduced surface. This outcome also proves the capability of the rotor illustrated in the first sections of generating friction forces usable for handling purposes and that its under-actuation is not limiting its functions, once one of the two external sources is exploited. In addition, from a quantitative perspective, the results show that for this specific application the sorting is reached using a limited space along the line and a short time, specifically at maximum $y_g \approx 2x_g$ and $t \approx 2.4\ s$, proving that this system is a compact and fast solution for the sorting problem in a transfer line.

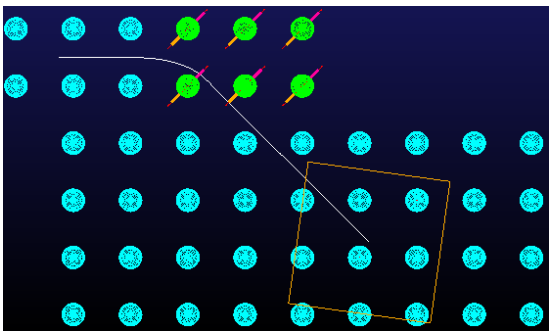

Figure 6. (Sorting trajectory of the center of mass and final position of the object with V_{x0}= 1 m/s as input condition.)

5. Conclusion

In this paper the authors present a new under–actuated surface for material handling purposes. The surface is composed by modules each one of them containing a spherical rotor with its axis of rotation temporarily defined by the contact with opposite pairs of pins. Furthermore, the inclination of the surface or the transported object initial velocity are exploited to compensate the missing actuation of the rotors. The paper include a brief introduction of the surface and of the rotor design, together with the analytical model of the latter. Then, a multi-body simulation is presented, at first, to validate the analytic model, and then, to calculate the results of the surface for the sorting activity using the two different actuation sources. First of all, from this section, emerged that the analytic model describes well the behaviour of the concept and that the errors between this and the simulated rotor are very limited. Secondly, the sorting simulations showed that the surface can be used for this task with the mentioned initial conditions. Furthermore, the outcomes provided relevant data to interpret the effect of these external sources of actuation, specifically about the sorting time and the space required. The latter were minimal, making the application of the surface within the transfer lines promising. As a future improvement could be interesting to realize the physical set-up and measure the real outcomes, but also extend both, the simulation and the test, to different handling applications.

Acknowledgements

This research work was undertaken in the con-text of DIGIMAN4.0 project ("Digital Manufacturing Technologies for Zero-defect", https://www.digiman4-0.mek.dtu.dk/). DIGIMAN4.0 is a European Training Net-work supported by Horizon 2020, the EU Framework Programme for Research and Innovation (Project ID: 814225).

References

[1] G Fantoni et al. Grasping devices and methods in automated production processes, *CIRP Annals* **63** (2014) 679–701.

[2] K-F B¨ohringer, V. Bhatt, B R Donald, K Goldberg, Algorithms for Sensorless Manipulation Using a Vibrating Surface, *Algorithmica*, Springer (2000).

[3] Chen, X; Zhong, W; Li, C; Fang, J; Liu, F, Development of a Contactless Air Conveyor System for Transporting and Positioning Planar Objects. *MDPI,Micromachines* 2018, **9**.

[4] Whiting, J; Mayne, R; Melhuish, C; Adamatzky, A, A Cilia-inspired Closed-loop Sensor-actuator Array. *J. Bionic Eng*. 2018, **15**, 526–532.

[5] Chen, Z; Deng, Z; Dhupia, J S; Stommel, M; Xu, W, Motion Modeling and Trajectory Tracking Control for a Soft Robotic Table. *IEEE/ASME Trans. Mechatron*. 2021, pp. 1–11.

[6] C I Rizescu, A I Ples, ea, D Rizescu, Modular Transport and Sorting System with Omnidirectional Wheels*, MATEC Web Conf.* (2021).

[7] Overmeyer, L; Ventz, K; and T Kruhn, S F, Interfaced multidirectional small-scaled modules for intralogistics operations. *Logist. Res.* 2010.